THE JOURNAL OF BIOLOGICAL CHEMISTRY VOL. 282, NO. 18, pp. 13250–13263, May 4, 2007


# Loss of Phylloquinone in *Chlamydomonas* Affects Plastoquinone Pool Size and Photosystem II Synthesis*[S]

Received for publication, November 2, 2006, and in revised form, February 21, 2007 Published, JBC Papers in Press, March 5, 2007, DOI 10.1074/jbc.M610249200

**Linnka Lefebvre-Legendre[‡], Fabrice Rappaport[§], Giovanni Finazzi[§], Mauro Ceol[‡], Chantal Grivet[¶], Gérard Hopfgartner[¶], and Jean-David Rochaix[‡1]**

*From the [‡]Departments of Molecular Biology and Plant Biology, University of Geneva, 30, Quai Ernest Ansermet 1211 Geneva 4, Switzerland, [§]Institut de Biologie Physico-chimique, UMR 7141 CNRS-Université Paris 6, 13 Rue Pierre et Marie Curie, 75005 Paris, France, and [¶]Life Sciences Mass Spectrometry, School of Pharmaceutical Sciences, University of Geneva, University of Lausanne, 20 Bd d'Yvoy, 1211 Geneva 4, Switzerland*

**Phylloquinone functions as the electron transfer cofactor at the $A_1$ site of photosystem I. We have isolated and characterized a mutant of *Chlamydomonas reinhardtii*, *menD1*, that is deficient in *MenD*, which encodes 2-succinyl-6-hydroxy-2,4-cyclohexadiene-1-carboxylate synthase, an enzyme that catalyzes the first specific step of the phylloquinone biosynthetic pathway. The mutant is photosynthetically active but light-sensitive. Analysis of total pigments by mass spectrometry reveals that phylloquinone is absent in *menD1*, but plastoquinone levels are not affected. This is further confirmed by the rescue of *menD1* by addition of phylloquinone to the growth medium. Analysis of electron transfer by absorption spectroscopy indicates that plastoquinone replaces phylloquinone in photosystem I and that electron transfer from $A_1$ to the iron-sulfur centers is slowed down at least 40-fold. Consistent with a replacement of phylloquinone by plastoquinone, the size of the free plastoquinone pool of *menD1* is reduced by 20–30%. In contrast to cyanobacterial *MenD*-deficient mutants, photosystem I accumulates normally in *menD1*, whereas the level of photosystem II declines. This decrease is because of reduced synthesis of the photosystem II core subunits. The relationship between plastoquinone occupancy of the $A_1$ site in photosystem I and the reduced accumulation of photosystem II is discussed.**

The photosystem II (PSII),[2] cytochrome $b_6f$, and photosystem I (PSI) complexes mediate the light-driven electron transport from water to ferredoxin in the thylakoid membrane of oxygenic photosynthetic organisms. These complexes consist of a large number of nucleus- and chloroplast-encoded subunits and numerous pigments and redox cofactors. Analysis of many mutants of *Chlamydomonas* deficient in photosynthetic activity has revealed that in general loss of any of the core subunits leads to the absence of the entire complex (1). However, in most cases the other complexes accumulate to normal levels. Most of the mutations that have been characterized affect genes encoding subunits of the complexes. Only a limited number of mutants deficient in the synthesis or assembly of the redox cofactors have been examined. In this respect, mutants of cyanobacteria and land plants deficient in phylloquinone synthesis have been characterized recently (2–7). Quinones play an important role as redox cofactors in PSII and PSI and as electron carriers between PSII and the cytochrome $b_6f$ complex.

The core of the PSII complex consists of the two reaction center polypeptides D1 and D2, the two peripheral antenna proteins CP43 and CP47, and several smaller polypeptides. D1 and D2 act as ligands for $P_{680}$, a chlorophyll dimer (8, 9) that is a strong oxidant capable of oxidizing water through Z identified as D1 amino acid Tyr-161 and the manganese cluster of the oxygen-evolving complex. D2 and D1 also form the terminal electron acceptor sites $Q_A$ and $Q_B$, respectively. Plastoquinone molecules function as fixed one electron cofactors at $Q_A$ or as two electron cofactors at $Q_B$, diffuse through the membrane, and are oxidized and deprotonated by the cytochrome $b_6f$ complex.

The photosystem I (PSI) complex is composed of five chloroplast-encoded and at least eight nucleus-encoded subunits (10). The two major subunits, PsaA and PsaB, contain 11 transmembrane domains and form the heterodimeric reaction center complex that coordinates the electron transfer cofactors. The primary electron donor $P_{700}$ consists of two chlorophyll *a* molecules and is located on the luminal side of the membrane. The primary electron acceptor, $A_0$, is a chlorophyll *a* monomer. The secondary electron acceptor $A_1$ is a phylloquinone molecule. There are two phylloquinones per $P_{700}$ corresponding to the two branches of the electron transfer chain, which converge on $F_X$, a [4Fe-4S] cluster in eukaryotes (11, 12). The question of whether in cyanobacteria most of the electrons are transferred asymmetrically along the PsaA branch is still debated (see 13, 14). From $F_X$ the electrons are transferred to the ultimate acceptors of PSI, the iron-sulfur centers $F_A$ and $F_B$ coordinated by the PsaC subunit located on the stromal side of the thylakoid membrane.

* This work was supported by Grant 3100-00667763.02 from the Swiss National Foundation. The costs of publication of this article were defrayed in part by the payment of page charges. This article must therefore be hereby marked "*advertisement*" in accordance with 18 U.S.C. Section 1734 solely to indicate this fact.

[S] The on-line version of this article (available at http://www.jbc.org) contains supplemental text, Figs. S1–S3, and Refs. 1–3.

[1] To whom correspondence should be addressed. Tel.: 41-22-379-6187; Fax: 41-379-6868; E-mail: Jean-David.Rochaix@molbio.unige.ch.

[2] The abbreviations used are: PSII, photosystem II; PSI, photosystem I; DBMIB, 2,5-dibromo-3-methyl-6isoporopyl-*p*-benzoquinone; DCMU, 3-(3,4-dichlorophenyl)-1,1-dimethylurea; LHC, light-harvesting system; SHCHC, 2-succinyl-6-hydroxy-2,4-cyclohexadiene-1-carboxylate; Chl, chlorophyll; LC-MS/MS, liquid chromatography-tandem mass spectrometry; ROS, reactive oxygen species; UTR, untranslated region; WT, wild type; PQ, plastoquinone.

The biosynthetic pathway of menaquinone has been elucidated in bacteria (15). Menaquinone and phylloquinone share the same naphthalene ring and differ in the phytyl side chain, which is an unsaturated C-40 chain in menaquinone and a mostly saturated C-20 chain in phylloquinone. By comparison of the genome of the cyanobacterium *Synechocystis* sp. PCC 6803 with bacterial genes, the enzymes involved in phylloquinone biosynthesis have been identified, and this pathway has been determined in cyanobacteria using reverse genetics (2, 3). It involves eight enzymes as follows: *menF* (isochorismate synthase), *menD* (2-succinyl-6-hydroxy-2,4-cyclohexadiene-1-carboxylate (SHCHC) synthase), *menC* (*o*-succinyl benzoate synthase), *menE* (*O*-succinylbenzoic acid-CoA synthase), *menB* (1,4-dihydroxy-2-naphtoyl-CoA synthase), *menH* (thioesterase), *menA* (1,4-dihydroxy-2-naphthoate phytyltransferase), and *menG* (methyltransferase). Loss of phylloquinone synthesis has different effects in cyanobacteria and land plants. In cyanobacteria, insertional inactivation of the *menA*, *-B*, *-D*, and *-E* genes leads to the complete absence of phylloquinone, which is replaced by plastoquinone-9 in PSI (2, 3, 16, 36). However, inactivation of *menG,* the last enzyme involved in the phylloquinone synthesis pathway, leads to the accumulation of demethylphylloquinone, which replaces phylloquinone in PSI (5). In these mutants the ratio between PSI and PSII is decreased. The mutants are still able to grow photoautotrophically under low light conditions at a slower rate in comparison with the wild type, and they are sensitive to high light. Mutants lacking phylloquinone have also been identified in *Arabidopsis thaliana*. Inactivation of *MenA* leads to a significant decrease of the PSI and PSII core subunits, and plastoquinone levels are reduced to 3% (6). Mutants affected at the *PHYLLO* locus, which encodes four *men*-homologous regions corresponding to *MenF*, *MenD*, *MenC,* and *MenH* genes, accumulate 5–15% of PSI and 55% of plastoquinone with nearly normal levels of PSII (7).

The biosynthetic pathway of phylloquinone biosynthesis has not yet been characterized in *Chlamydomonas reinhardtii*. Here we describe the identification and characterization of *menD1*, a nuclear insertion mutant of *C. reinhardtii*, which was identified during a screen for mutants impaired in state transitions, a process that leads to the lateral redistribution of the LHCII antenna along the thylakoid membrane and to their preferential association with PSII (state 1) or PSI (state 2). This redistribution of LHCII is accompanied by significant changes in the maximum fluorescence yield, and these changes set the basis of a screen allowing one to identify mutants affected in state transitions (17, 18). Our analysis shows that the fluorescence phenotype is in fact indicative of a deficiency in the biosynthesis of phylloquinone because of the inactivation of a gene corresponding to the *menD* gene. Although the absence of phylloquinone biosynthesis appears to lead, as in the case of cyanobacteria, to its replacement by plastoquinone in PSI, the secondary effects are rather different. We show that the accumulation of PSI subunits is not affected in the *menD1* mutant but that the absence of phylloquinone leads to a decrease in size of the free plastoquinone pool together with a reduced synthesis of PSII subunits.

## EXPERIMENTAL PROCEDURES

*Strains and Media—C. reinhardtii* wild type, *arg7*, *arg2*, *QDO*, a cytochrome $b_6f$-deficient mutant (42), and the double mutant strain *KRC1003* (*nac2 P71*) (19) lacking PSII and containing decreased amounts of light-harvesting complexes were grown as described (20). If necessary, the acetate-containing medium (TAP) was supplemented with either $10^{-5}$ M 3-(3,4-dichlorophenyl)-1,1-dimethylurea (DCMU) (ICN Biochemicals), $10^{-2}$ mg/ml paromomycin sulfate (Sigma), $2 \times 10^{-6}$ M 2,5-dibromo-3-methyl-6-isopropyl-*p*-benzoquinone (DBMIB) (Sigma), 200 $\mu$g/ml chloramphenicol (Fluka), or with 5 $\mu$M phylloquinone (Sigma). Crosses were performed using standard protocols (20). Transformations were achieved using the glass beads/vortex protocol (21). The pSL17 plasmid[3] containing the *AphVIII* gene conferring paromomycin resistance was used to transform wild-type cells. Incubation bags Anaerocult P (Merck) were used for growth under reduced oxygen levels.

*Characterization of the MenD1 Gene*—DNA manipulations and cloning were carried out using standard procedures (22). For DNA gel blot analyses, wild-type and *menD1* DNA were digested with KpnI or NcoI enzymes. A fragment BstBI-SalI of the *AphVIII* gene was used as a probe.

DNA walking was performed according to the user manual of Clontech. Genomic DNA was extracted as described (23) and digested with NaeI restriction endonuclease that creates blunt ends. Digested DNA was then ligated to an adaptor. A first PCR was performed using GWFor1 primer specific of the transformation vector (pSL17) (GWFor1, 5′-ACTTGGTCTGACAGTTACCAATGC-3′) and AP1 primer specific of the adaptor (AP1, 5′-GTAATACGACTCACTATAGAGT-3′). The first PCR products were then used as a template for a second PCR using the AP2 primer (AP2, 5′-ACTATAGAGTACGCGTGGT-3′) and the GWFor2 primer specific of pSL17 (GWFor2, 5′-CGTTCATCCATAGTTGCCTGACTC-3′).

Analysis of the plasmid insertion was performed by PCR on DNA extracted as described (24), and the following oligonucleotides were used: E4down (5′-GTGAAGCCGCCGAAGATCTTG-3′); E3up (5′-TGACCAGCAGCGGCACCGCCGTGGCCA-3′); E4up (5′-AAGATCTTCGGCGGCTTCACGCGCT-3′); postE4down (5′-ACACATGCACACACGCACACA-3′); GWFor1 (5′-ACTTGGTCTGACAGTTACCAATGC-3′); E9up (5′-TGTACGTGGCGCCGCACACGCTGC-3′); E10down (5′-ATGTCCCGAATGGGCATGGAG-3′); E12up (5′-CATTGACGGCGTGCTGTCGAC-3′); E13down (5′-CACAGCGGCGTGAACTCGTTCTCG-3′); E15up (5′-ACGTCCACGCCCTGGCCCGCATGA-3′); and E15down (5′-CCGCCAGCCGCCCGTCAGGCCACGTCA-3′).

The fragment obtained by DNA walking was used to screen a cosmid library. The C4–119A cosmid was digested with BamHI restriction endonuclease, and a fragment of ~6.5 kb was subcloned in the plasmid vector pBluescript KS+ (Stratagene, La Jolla, CA). The resulting plasmid was called pKS/IB.

Total RNA was extracted from *C. reinhardtii* cells and treated with DNase I using RNeasy plant mini kit from Qiagen.

[3] S. Lemaire and J. D. Rochaix, unpublished results.

Reverse transcription was performed using random primers (Promega) and SuperScript II RT (Invitrogen).

For PCRs, the following oligonucleotides were used: E1E2down (5′-CGAGGAGCGGGAGCCCGGCGCCACTGC-3′); 5′-UTRup3 (5′-GCGTGCAATAGAATGAGGACA-3′); E2down (5′-TCGTCAATGCACACGTTGAGG-3′); E1up (5′-GTCAACATGTTCGCAGTGGCG-3′); E3down (5′-TGTGT-CGGCGGTTGGTCTGGTAGCTGG-3′); E2up (5′-CCTCA-ACGTGTGCATTGACGA-3′); E4down (5′-GTGAAGCCGC-CGAAGATCTTG-3′); E3up (5′-TGACCAGCAGCGGCAC-CGCCGTGGCCA-3′); E8down (5′-GACAGCACGTCCGCC-ACCACCGGCCAG-3′); E4up (5′-CTTCACGCGCTGGTTC-TTCGACCT-3′); E8up (5′-ATCTGCGCCGCGCTGGGCTG-GCCGGT-3′); E9down (5′-GGTCCATGACCGCCCGGTGT-GAGACCA-3′); E9up (5′-CCCACCTGGTCTCACACCGGG-CGGTCA-3′); E10down (5′-CGGGCCAAGCTGCGCGCGAT-GAAGGGC-3′); E10up (5′-CTCCATGCCCATTCGGGACAT-3′); E11down (5′-GCAGTCGACAGCACGCCGTCAATG-3′); E11up (5′-CATTGACGGCGTGCTGTCGAC-3′); E15up (5′-TCATGCGGGCCAGGGCGTGGACGTGCT-3′); E15down (5′-CCGCCAGCCGCCCGTCAGGCCACGTCA-3′); E14up (5′-CAGTGTGGTGGAGGTGGTCACGGA-3′); E15up (5′-ACGTCCACGCCCTGGCCCGCATGA-3′); and 3′-UTRdown (5′-CGGGATGAGGCGAGCAGGGCA-3′).

*Optical Spectroscopy in Vivo*—For spectroscopic measurements, cells were harvested during exponential growth (~$2 \times 10^6$ cells $ml^{-1}$) and resuspended in minimum high salt medium with the addition of Ficoll 20% (w/v) to prevent cell sedimentation. Measurements were done on intact cells at a chlorophyll concentration of ~70 $\mu$g of Chl $ml^{-1}$. Spectroscopic analysis was performed at room temperature, using a homemade pump and probe spectrophotometers. Two different setups were employed. The absorption changes were measured using a spectrophotometer in which short monochromatic flashes are generated by an Nd:YAG pumped optical parametric oscillator. A tunable dye laser pumped by the second harmonic of an Nd:YAG laser was used to excite the sample at 700 nm. This setup has a high signal to noise ratio and a time resolution of 10 ns (25).

Cytochrome *f* oxidation kinetics (Fig. 5*B*) were measured with a LED-based spectrophotometer, as described elsewhere (26). Actinic flashes were provided by a dye laser at 690 nm, and measuring flashes were provided by a white LED (Luxeon, Lumileds, CA), filtered with interference filters (10 nm full width at half-maximum). Cytochrome *f* redox changes were calculated as the difference between the absorption at 554 nm and a base line drawn between 545 and 573 nm (27) and corrected for the contribution of the electrochromic signal (5% of the signal observed at 515 nm) (28).

*Measurements of PSI and PSII Activity*—PSII/PSI charge separation was measured as the extent of the electrochromic signal at 515–545 nm, 100 $\mu$s after excitation with a single turnover laser pulse at 695 nm. This signal is linearly proportional to reaction center photochemistry (29). PSII contribution was deduced as the difference between the signals measured in the absence and presence of the PSII inhibitors DCMU and hydroxylamine (30). The latter compound was added to destroy the manganese cluster responsible for oxygen evolution and to slow down recombination between the donor and acceptor side of PSII, which would preclude correct estimation of the PSI/PSII ratio.

PSI activity was also determined by measuring light-induced oxygen uptake with a Clark-type oxygen electrode (Hansatech) at 25 °C. The reaction mixture contained cells broken by sonication (30 $\mu$g chlorophyll/ml) in 50 mM Hepes-KOH, pH 7.5, 5 mM NaCl, 5 mM $MgCl_2$, 2 mM $NH_4Cl$, 3 mM $Na_3N$, 0.2 mM methyl viologen, 1 mM sodium ascorbate, 0.2 mM 2,6-dichlorophenolindophenol, and 10 $\mu$M DCMU. PSII activity was determined by measuring light-induced oxygen evolution in whole cells (10 $\mu$g of chlorophyll/ml) in 50 mM Hepes-KOH, pH 7.5, 5 mM NaCl, 5 mM $MgCl_2$, 0.2 mM phenyl-*p*-benzoquinone, 2 $\mu$M DBMIB.

*Fluorescence Measurements*—To screen for state transition mutants, state transitions were measured as described (17). *C. reinhardtii* cells were grown on TAP plates supplemented with $10^{-5}$ M DCMU. State 1 (associated with high fluorescence at room temperature) was obtained by oxidation of the plastoquinone pool by illumination of the plates with white light (60 $\mu$E $m^{-2}$ $s^{-1}$) for 15 min. State 2 (associated with low fluorescence at room temperature) was induced by reducing the plastoquinone pool by flushing the plates with nitrogen in the absence of light. Fluorescence pictures of the whole plate corresponding to state 1 and state 2 were recorded, quantified, and subtracted numerically. The differential fluorescence signal of each colony provides a measure of state transition.

Fluorescence kinetics were measured with a home-built setup, in which cells were excited with green light at 520 nm (Luxeon, Lumileds), and emission was measured in the near far red (60). The size of the plastoquinone pool was estimated from induction kinetics in mutant cells lacking the cytochrome $b_6f$ complex as the ratio between the area above the fluorescence curve measured in the absence and presence of the PSII inhibitor DCMU (see "Results").

*Measurements by Mass Spectrometry*—Thylakoid membranes were isolated as described (31). The pigments were extracted as described (37), sequentially with 1 ml of methanol, 1 ml of 1:1 (v/v) methanol/acetone, and 1 ml of acetone, and the three extracts were combined, and the resulting solution was concentrated by vacuum. The pigments were resuspended in a mixture of 1:1 methanol/isopropyl alcohol at 0.77 mg of Chl $ml^{-1}$. Their pigment composition was measured by liquid chromatography coupled with tandem mass spectrometry (LC-MS/MS) using atmospheric pressure chemical ionization. The analytes were separated on a 150 × 4.6 mm Novapack C18 column (Waters) using a high pressure gradient pump system at a flow rate of 1 ml/min (Shimadzu, Reinach, Switzerland). The gradient started with 10% solvent B for 1 min and was increased to 90% B in 15 min. 90% solvent B was maintained for a further 14 min. Solvent A was a mixture of methanol/water at a ratio of 9:1 (v/v), and solvent B was composed of a mixture of methanol/isopropyl alcohol at a ratio of 7:3 (v/v). The injection volume was 10 $\mu$l. A UV detector operated at $\lambda = 254$ nm (Shimadzu) was placed prior to MS detection. Phylloquinone and plastoquinone eluted at room temperature for 13.7 and 18.8 min, respectively. Mass spectrometric detection was performed on a triple quadrupole linear ion trap (Q Trap 4000,

AB/MDS Sciex, Canada). Ionization of the analytes was achieved using atmospheric pressure chemical ionization. Phylloquinone and plastoquinone concentrations were measured in the positive selected reaction monitoring mode using the following transition: $m/z$ 451 > $m/z$ 128 (CE = 90 eV) and $m/z$ 749 > $m/z$ 151 (CE = 110 eV), respectively. Nitrogen was used as collision gas. Confirmatory analysis was performed using enhanced full scan MS and enhanced product ion scan.

*Protein Extracts and Immunoblot Analysis*—Total cell extracts were prepared as described (32). For immunoblot analysis, proteins were fractionated on 12% SDS-PAGE and immunoblotted with the specific antiserum. The antisera used in this work were α-PsaA (1:5000), α-D1 (1:4000), α-D2 (1:5000), α-CP47 (1:25,000), α-Oee1 (1:5000), α-Oee2 (1:5000), α-Oee3 (1:5000), α-Cytf (1:4000), α-LHCI (1:10,000), α-LHCII (1:2000), α-PsaD (1:1000), α-PsaF (1:4000), α-RbcL (1:20,000), and α-α$CF_1$ (1:5000). The ECL immunoblotting system (33) was used to detect the immunoreactive proteins with anti-rabbit or anti-chicken secondary antibodies.

*RNA Blot Analysis*—RNA blot analysis was performed as described (34). The full-length cDNA of *psbA* was used as a probe.

*Pulse Labeling of Chloroplast-encoded Proteins*—Protein pulse-labeling experiments were performed as described (35).

## RESULTS

*Growth and Fluorescence Properties of the menD1 Mutant*—The *menD1* mutant was isolated during a screen for *C. reinhardtii* cells deficient in state transitions. Insertional mutagenesis was achieved by transformation of wild-type cells with the pSL17 plasmid conferring paromomycin resistance. Although *menD1* was originally identified as a mutant deficient in state transitions, further analysis did not confirm this phenotype (supplemental Fig. S1). Fig. 1*A* shows that the mutant grows as well as the wild type on acetate medium (TAP) in the dark and at light intensities of 6 and 60 $\mu E\ m^{-2}\ s^{-1}$. However, the *menD1* mutant is unable to grow under high light (600 $\mu E\ m^{-2}\ s^{-1}$) and grows poorly in the absence of acetate on minimal medium (HSM). The mutant is photosynthetically active as revealed by the fluorescence transients at room temperature of dark-adapted wild-type and mutant cells in the absence or presence of DCMU, a PSII inhibitor that blocks $Q_A^-$ reoxidation and thus allows one to measure the maximum fluorescence yield ($F_{max}$). As shown in Fig. 1*B*, for cells grown under 60 $\mu E\ m^{-2}\ s^{-1}$ light, the steady state fluorescence yield reached after a few seconds of continuous illumination ($F_{stat}$) was lower than $F_{max}$, indicating that PSII sustains a significant electron flux in the mutant. Yet the difference ($F_{max} - F_{stat}$) was smaller in the *menD1* mutant than in the control strain indicating a decreased PSII photochemical efficiency. Similar patterns were observed under 6 $\mu E\ m^{-2}\ s^{-1}$ light; the *menD1* mutant had a higher $F_0$ resulting in a lower $F_V/F_M$ value of 0.66 ± 0.01 as compared with 0.83 ± 0.01 for the wild type, suggesting a decrease in the amount of functional PSII.

The striking contrast between the poor growth of *menD1* on minimal medium and its almost normal photosynthetic electron flow (Fig. 1, *A* and *B*) suggested that the impairment of growth may be an indirect effect of the primary lesion, which could lead to the formation of reactive oxygen species (ROS). To test this possibility *menD1* cells were grown under lower oxygen pressure. As seen in Fig. 1*A*, photoautotrophic growth was restored, strongly suggesting that the poor growth of *menD1* is due, at least in part, to photooxidative damage. Growth on acetate under high light (400 $\mu E\ m^{-2}\ s^{-1}$) could also be restored in the presence of DCMU, indicating that the damage was linked to photosynthetic electron flow (Fig. 1*A*).

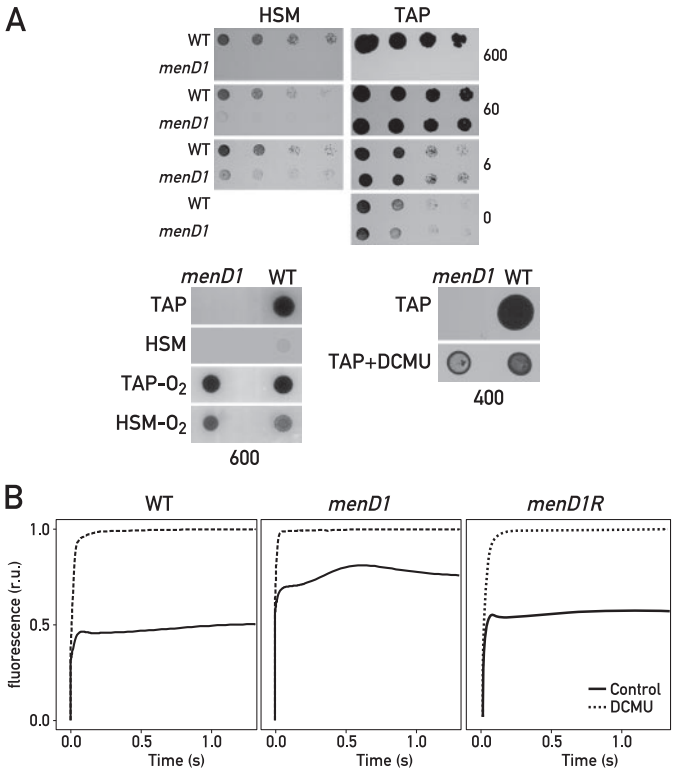


FIGURE 1. *A,* growth patterns of wild type and *menD1* on minimal (HSM) or acetate-containing medium (TAP). 10 μl of cell culture at 3 × $10^6$ cells/ml were spotted with 1:5 series dilution on agar plates and grown under 0, 6, 60, 400, and 600 $\mu E\ m^{-2}\ s^{-1}$ light as indicated. Cells were also grown under reduced oxygen pressure ($-O_2$) or in the presence of DCMU. *B,* fluorescence transients of wild type, *menD1,* and the complemented strain *menD1R* in the presence or absence of DCMU under 60 $\mu E\ m^{-2}\ s^{-1}$ light.

*Cloning of the MenD Gene*—DNA blot analysis with wild-type and *menD1* genomic DNA carried out with a pSL17-specific probe showed that the *menD1* mutant contained a single copy of the pSL17 plasmid in the genome (Fig. 2*A*). To test whether the phenotypes of the *menD1* mutant were linked to the plasmid insertion, a backcross with a wild-type strain was performed from which 21 complete tetrads were recovered. Analysis of the progeny revealed a cosegregation of the growth impairment and paromomycin resistance, indicating that the mutant was tagged. Furthermore, analysis of diploids obtained by crossing the *menD1*;*arg7* double mutant with an *arg2* mutant revealed that the *menD1* mutation is recessive, suggesting a loss of function.

Because the *menD1* mutant is tagged, it was possible to identify the sequences flanking the transformation vector by PCR (see "Materials and Methods"). This method allowed us to amplify one of the flanking regions. The other flanking region could not be identified using the same approach, probably because of rearrangements of the vector sequences during the

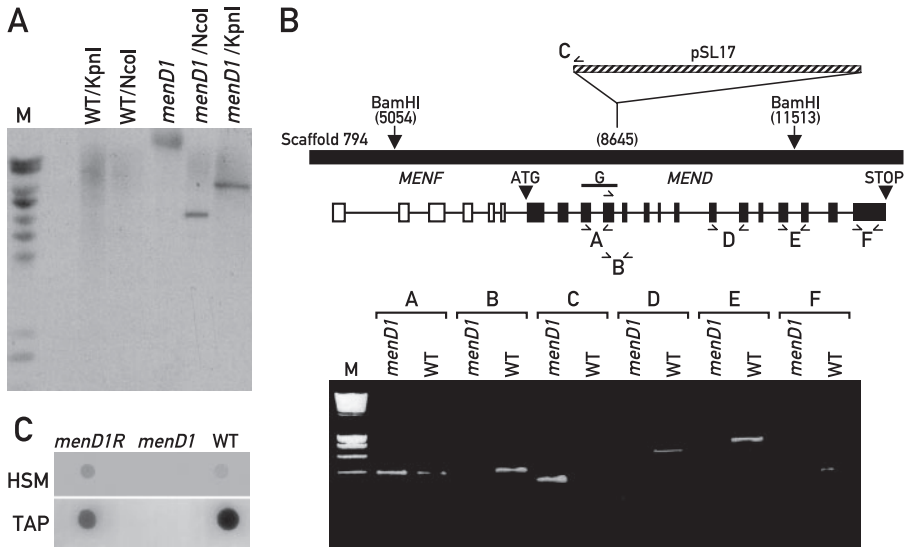


FIGURE 2. *A,* the *menD1* mutant contains a single insertion of the paromomycin cassette. DNA from wild-type and *menD1* cells was extracted, digested with restriction enzymes as indicated, fractionated by electrophoresis on an agarose gel, blotted onto a Hybond filter, and hybridized with a probe of the paromomycin cassette used for generating *menD1*. *B, upper,* organization and structure of the *MenF* and *MenD* genes of *Chlamydomonas*. Exons of *MenF* and *MenD* are indicated by *open* and *black boxes*, respectively. *Lower,* ethidium bromide staining of PCRs performed on DNA from wild type and *menD1* with the indicated primer pairs A–G. *C,* complementation of *menD1* with the *MenD* gene of *C. reinhardtii*. Cells from the complemented strain *menD1R*, *menD1*, and wild type were spotted on HSM and TAP medium under 600 $\mu$E $m^{-2}$ $s^{-1}$ light. *Lane M* indicates DNA size markers.

integration event. A BLAST search of the PCR product on the *Chlamydomonas* nuclear genome sequence (version 1.0) revealed that the pSL17 vector was inserted in the region corresponding to scaffold 794 at position 8645. To further characterize the insertion site of the transforming DNA, PCR analysis with different primers was performed. As expected, it was possible to amplify the region upstream of position 8645 with both *menD1* and wild-type genomic DNA (PCR A, Fig. 2*B*). Using primers flanking position 8645, a PCR product was obtained with wild-type DNA but not with mutant DNA because the insertion prevented any amplification (PCR B, Fig. 2*B*). As expected, amplification was possible only with *menD1* DNA when a primer annealing with the plasmid and a primer in the flanking region were used (PCR C, Fig. 2*B*). Furthermore, by using different sets of primers to amplify regions downstream of the plasmid insertion site, PCR products were obtained with wild-type DNA but not with the DNA of *menD1* (PCR D, -E, and -F, Fig. 2*B*), indicating that a large deletion had occurred in this region of the genome of *menD1*. This deletion was confirmed by DNA blot analysis. Wild-type genomic DNA was digested with NcoI, which produced a fragment of ~4000 bp that hybridizes with the PCR D probe. In contrast, no specific hybridization could be obtained with *menD1* genomic DNA treated in the same way (data not shown).

To confirm that the region near the insertion site contains the gene whose inactivation is responsible for the phenotype of *menD1*, genomic complementation was performed. The PCR G fragment (Fig. 2*B*) was used as a probe for isolating a cosmid from a wild-type library. This cosmid, named C4–119A, ~35 kb long, was used to transform *menD1* by selecting for growth under high light (600 $\mu$E $m^{-2}$ $s^{-1}$). Transformants able to grow under high light were obtained readily, whereas no transformant was obtained in a control transformation without DNA, thus indicating that the C4–119A cosmid contains the wild-type gene affected in the *menD1* mutant. A BamHI fragment of 6.5 kb containing the region interrupted by the insertion in *menD1* (from positions 5054 to 11,513 on scaffold 794, Fig. 2*B*) was subcloned giving rise to plasmid pKS/IB. It was also able to rescue the *menD1* mutant by transformation. The transformants obtained were able to grow under high light on both acetate and minimal media. The growth patterns of one of them, *menD1R*, are shown in Fig. 2*C*. In this transformant the wild-type fluorescence patterns were restored (Fig. 1*B*).

The 6.5-kb BamHI fragment contains the 3′ end of *MenF* (positions 3994 and 7024 in Fig. 2*B*) and most of *MenD* (starting at 7414). A large deletion occurred in the *MenD* gene in the *menD1* mutant. The *MenC* and *MenH* genes are located close to *MenD*. Thus, these four *Men* genes involved in phylloquinone synthesis are localized close to each other as in *Arabidopsis*. However, it is not clear whether they are coexpressed in *C. reinhardtii* in a single transcription unit as the *PHYLLO* locus in *Arabidopsis* (7). The only known function of phylloquinone in cyanobacteria and plants is to act as an electron transfer cofactor in PSI.

Because no expressed sequence tags from *C. reinhardtii* corresponding to *MenD* are available in the data bases, a cDNA library was screened using the PCR G fragment already used to isolate the C4–119A cosmid. No corresponding cDNA was obtained among 200,000 phages screened. Taken together, the absence of expressed sequence tags and cDNAs suggests that the *MenD* gene is poorly expressed. Because the available genomic sequence of *MenD* did not reveal start and stop codons, reverse transcription-PCR was performed to determine the cDNA sequence of *MenD*. Because amplification of the complete cDNA from the poly(A) sequence was not possible, reverse transcription was performed using random hexamers. PCR amplifications were done using different sets of primers designed according to the exons predicted by the genewise model. A cDNA fragment was obtained using a primer annealing to the putative 5′-UTR region of the *MenD* gene and a primer spanning the putative exons 1 and 2. Sequencing of this fragment showed the presence of a stop codon in the same reading frame as *MenD*, 33 bp upstream of the first ATG. This result suggests that the MenF and MenD proteins are expressed independently. Reverse transcription-PCR revealed an in-frame stop codon at position 12,985. According to our sequence data and those of JGI, the complete cDNA of *MenD* contains 15 exons and 14 introns (accession number DQ445258). The deduced *MenD* open reading frame encodes

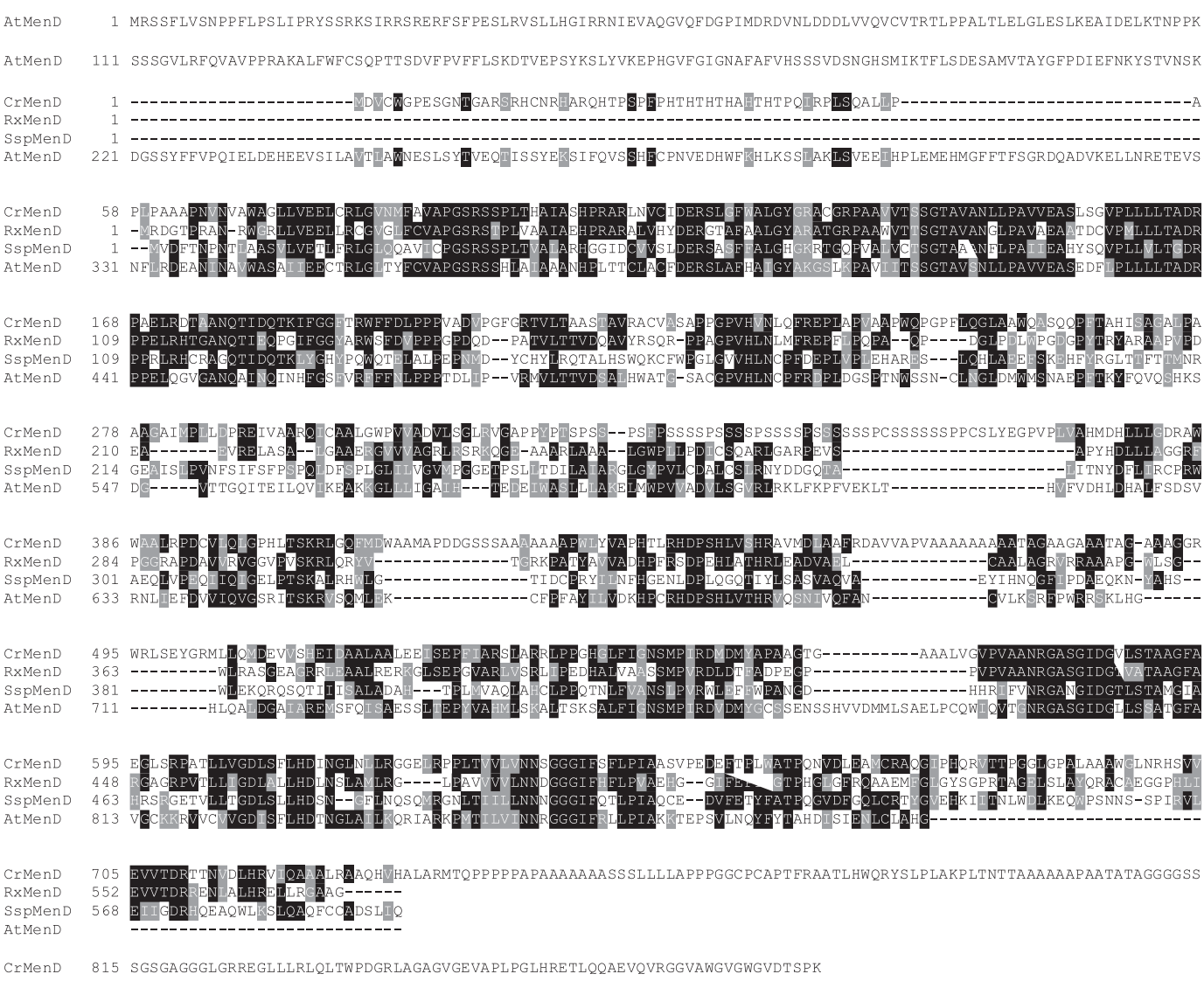


FIGURE 3. **Sequence comparison of MenD protein from *C. reinhardtii* (CrMenD), *A. thaliana* (AtMenD), *R. xyanophilus* DSM 9941 (RxMenD), and *Synechocystis* PCC 6803 (SspMenD).** AtMenD is part of the PHYLLO protein (7). The protein sequences were aligned using ClustalW (59) and boxshade.

an 885 amino acid protein of 90,708 Da with a pI of 9.34. The protein contains two domains conserved in the SHCHC synthase, residues 65–320 and 370–676. The pKS/IB plasmid that complements the *menD1* mutant encodes the first 637 amino acids of the MenD protein, indicating that the C-terminal end of the MenD protein is most likely dispensable for its function.

Fig. 3 displays an alignment between the MenD protein of *C. reinhardtii* and its orthologues in *A. thaliana,* in the cyanobacterium *Synechocystis* sp. PCC 6803, and in *Rubrobacter xylanophilus* DSM 9941. The C-terminal ends of the MenD proteins are very divergent, which suggests that they are not important for the function. This could explain why the complementation of the *menD1* mutant was observed with a C-terminal truncated protein. The *Chlamydomonas* MenD protein displays 24% sequence identity to the MenD protein (SHCHC synthase) of *Synechocystis* sp. PCC 6803. Inactivation of the *MenD* gene in *Synechocystis* sp. PCC 6803 was shown to lead to the loss of phylloquinone indicating that there is no alternative pathway in cyanobacteria.

*The menD1 Mutant Is Affected in the Biosynthetic Pathway of Phylloquinone*—If the *MenD* gene of *C. reinhardtii* encodes the SHCHC synthase required for phylloquinone synthesis, one would predict that it is possible to restore the growth of the *menD1* mutant under high light by supplementing the medium with phylloquinone. Indeed, addition of phylloquinone allows for the growth of the *menD1* mutant under high light (Fig. 4*A*) confirming that the *menD1* mutant is affected in phylloquinone biosynthesis. Addition of 1,4-dihydroxy-2-naphthoate, an intermediate in phylloquinone biosynthesis that acts downstream of MenD, also partially restores growth of *menD1* under high light (Fig. 4*A*). For unknown reasons restoration of growth by these compounds was only possible on agar plates and not in liquid medium.

It was shown that in the *Synechocystis* sp. PCC 6803 *menD*-deficient mutant, the missing phylloquinone is replaced by plastoquinone-9, which acts as a substitute for phylloquinone and mediates electron transfer from $A_0$ to $F_X$ (36). Consequently, the PSI complex is functional. However, the PSI content is lower than in wild-type cells, and the mutant grows more

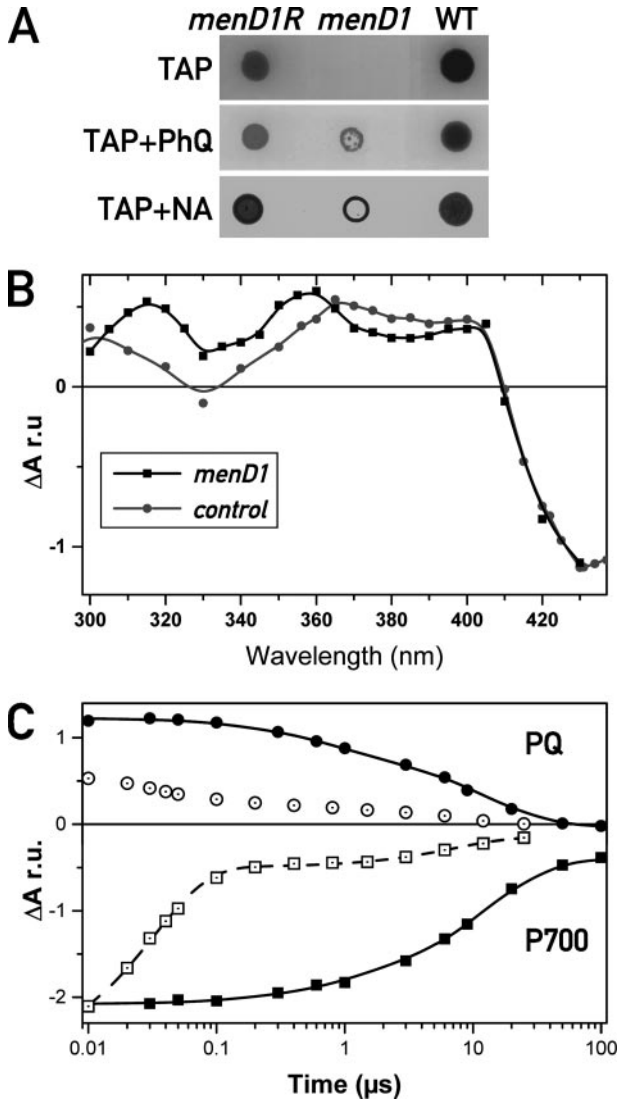


FIGURE 4. *A,* addition of phylloquinone or 1,4-dihydroxy-2-naphthoate restores growth of menD1 in the light (600 $\mu$E $m^{-2}$ $s^{-1}$). Cells were spotted on TAP medium or on TAP medium supplemented with phylloquinone or 1,4-dihydroxy-2-naphthoate (*NA*). *B,* absorption spectrum of cells from the *KRC1003* and *menD1-KRC1003* strains measured 10 ns after a flash. *C,* kinetics of 320 and 430 nm absorption changes induced by a flash of *menD1-KRC1003* cells corresponding to the oxidation of plastosemiquinone (*circles*) and the reduction of $P_{700}^+$ (*squares*), respectively, under aerobic (*dark symbols*) and anaerobic conditions (*open symbols*).

slowly than the wild type under normal light, and it is unable to grow under high light conditions (36).

To assess whether PSI function was also affected in the *menD1* mutant, we characterized electron transfer in PSI *in vivo* using absorption spectroscopy. To reduce the background noise because of PSII and the antennae, the *menD1* mutant was crossed with *KRC1003*, a strain lacking PSII and containing decreased amounts of light-harvesting complexes (19). As shown in Fig. 4*B* the spectra of the absorption changes measured 10 ns after a flash in intact cells of *menD1-KRC1003* and of the control *KRC1003* were different. In the control strain, the pronounced bleaching at 430 nm and absorption increase in the 360–390 nm region are characteristic for $P_{700}^+$ and $A_1^-$, respectively. Although the absorption changes observed in the 430 nm region were similar in both cases, indicating that the ($P_{700}^+$–$P_{700}$) spectrum was not affected by the mutations, they were significantly different in the 300–360 nm region. In particular, a pronounced absorption increase peaking at ~320 nm was specifically observed in the mutant, consistent with the expected absorption changes associated with plastoquinone reduction (37). Taken together, these data indicate that, as in *Synechocystis* sp. PCC 6803, plastoquinone may occupy the phylloquinone site in PSI and serve as an electron carrier.

The rate of oxidation of plastosemiquinone in *menD1* was estimated by determining the kinetics of the absorption changes at 320 nm following a flash. This signal decayed with a half-time of ~6 $\mu$s, which is significantly slower than the values measured in the WT ($t_{1/2}$ of ~20 and 150 ns (11, 12)) but similar to the decay of $P_{700}^+$ which is, itself, consistent with the known electron transfer rate from plastocyanin to $P_{700}^+$ (Fig. 4*C*). To exclude the possibility that the coincidence between these two half-times is because of charge recombination between plastosemiquinone and $P_{700}^+$, the electrochromic band shift induced by the electric field across the membrane was measured 100 $\mu$s after the actinic flash. The amplitude of the signal was found to be similar in the wild-type and mutant strains (data not shown), indicating that the lifetime of the charge separated state is longer than 6 $\mu$s.

The results obtained after a long period of anaerobiosis (more than 60 min) were markedly different. The relative absorption changes observed at 320 nm were strongly decreased, suggesting a decreased yield in plastoquinone reduction, whereas the overall absorption changes ascribed to $P_{700}^+$ were unchanged in amplitude but decayed with a half-time of ~25 ns (rather than 6 $\mu$s under aerobic conditions). A similar half-time was found when studying the $P_{700}^+A_0^-$ radical pair decay by charge recombination (38, 39). This, together with the diminished absorption changes resulting from plastoquinone reduction, suggests that under such conditions forward electron transfer from $A_0^-$ is blocked in a significant fraction of centers, and charge recombination occurs. Consistent with this, the amplitude of the electrochromic band shift resulting from charge separation, measured 100 $\mu$s after a flash, decreased after prolonged anaerobiosis (data not shown).

*The Size of the Free Plastoquinone Pool Is Altered in the menD1 Mutant*—To confirm the loss of phylloquinone in PSI centers of *menD1*, the pigments of thylakoid membranes from the mutant and the wild-type strain were extracted. The pigment composition was determined by LC-MS/MS. Isolated phylloquinone and plastoquinone were used as internal standards for identifying the fractions corresponding to these molecules and for their quantitation during analysis by LC-MS/MS. The selected reaction monitoring mode was used for the estimation of concentrations. For confirmatory analysis full scan single MS and enhanced product ion experiments, in the trap mode, were performed. The obtained product ion spectra were in good accordance with those obtained with the reference compounds. In full scan mode and at the retention time of phylloquinone and plastoquinone, no coeluting analytes were observed. Also standard addition of reference compounds to the extracts did not result in any deformation of the chromatographic peaks. In this way peaks corresponding to plastoquinone and phylloquinone could be clearly identified in wild-type

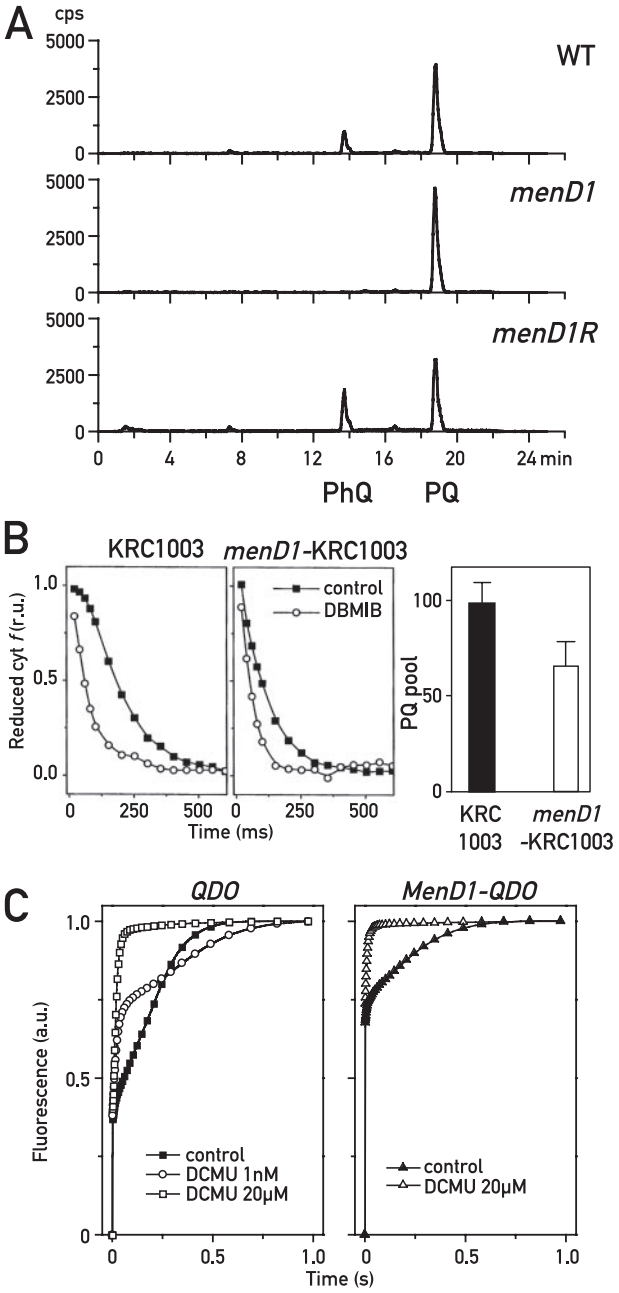


FIGURE 5. *A,* mass spectrometric analysis (selected reaction monitoring mode) of phylloquinone (*PhQ*) and plastoquinone (*PQ*) from wild type, *menD1*, and the complemented strain *menD1R*.; *cps*, counts/s. *B,* size of plastoquinone pool is reduced in *menD1*. The absorption changes associated with the oxidation of cytochrome *f* were measured in the presence or absence of 2 μM DBMIB in intact cells of *KRC1003* (control) or of *menD1-KRC1003*. The relative sizes of the free plastoquinone pool are shown. *C,* fluorescence transients of *QDO* (lacking the cytochrome $b_6f$ complex) and *menD1-QDO* in the presence and absence of DCMU. *Symbols, left panel,* control sample QDO, *solid squares*; 20 μM DCMU, *open squares*; 1 nM DCMU, *open circles*. *Right panel, menD1-QDO* cells, *triangles*; 20 μM DCMU, *open triangles*. The PQ/PSII ratios were 5.7 ± 0.7 in untreated *QDO* cells, 10.5 ± 0.5 in *QDO* cells treated with 1 nM DCMU, and 8.7 ± 0.7 in *menD1-QDO* cells.

extracts. In contrast, *menD1* extracts were found to lack phylloquinone, whereas no significant change in the level of plastoquinone was observed compared with the wild type (Fig. 5*A*). Using purified plastoquinone and phylloquinone as standards, the amount of plastoquinone (PQ) was estimated from two independent measurements at 5.1 ± 0.5, 5.6 ± 0.5, and 3.9 ± 0.5 μmol of PQ/mmol of Chl in the wild-type, *menD1,* and *menD1R* complemented strain, respectively. The amount of phylloquinone was estimated at 1.1 ± 0.4 and 1.4 ± 0.5 μmol of phylloquinone/mmol of Chl in the wild type and in *menDR1*, respectively, thus indicating that the level of phylloquinone is restored in the complemented strain (Fig. 5*A*). These results thus confirm that there is a defect in the phylloquinone biosynthetic pathway in the *menD1* mutant and that there is only one pathway for producing phylloquinone in *C. reinhardtii* as in *Synechocystis* sp. PCC 6803. In addition, these measurements indicate that the total content of plastoquinone in the mutant is the same as in the wild type.

Although the amount of plastoquinone is the same in the WT and the *menD1* mutant, the size of the free plastoquinone pool in the photosynthetic electron transport chain might be reduced in the latter if plastoquinone replaces phylloquinone in the PSI complex. To test this possibility, we estimated the size of the plastoquinone pool in the two strains by measuring the kinetics of cytochrome *f* oxidation under continuous light. We used the mutant strains *KRC1003* and *menD1-KRC1003* containing reduced levels of light-harvesting complexes and lacking PSII. Thus, reduction of the plastoquinone pool is blocked in the light and illumination results in the complete oxidation of cytochrome *f* by PSI, with a rate that is determined both by the light intensity and by the number of reduced electron carriers available for cytochrome *f* reduction.

Fig. 5*B* shows the kinetics of cytochrome *f* oxidation measured in *KRC1003* and *menD1-KRC1003*. These experiments were performed under anaerobic conditions, to completely reduce the electron carriers upstream of cytochrome *f* in the electron transport chain because of the rather negative cellular redox potential. Yet the incubation time was kept short enough to avoid charge recombination at the level of PSI (see above). In *Chlamydomonas*, anaerobic conditions induce a switch from linear to cyclic electron flow mediated by state transitions (28, 40). Cyclic electron flow involves the reinjection of reducing equivalents produced by PSI into the plastoquinone pool. This phenomenon, which can blur the determination of the size of the plastoquinone pool, can be avoided in low antenna strains (40), as the *KRC1003* and *menD1-KRC1003* strains employed in this experiment. We thus obtained a full oxidation of cytochrome *f* under continuous illumination as shown by the comparison of the absorption changes resulting from cytochrome *f* oxidation in the absence and presence of DBMIB, an inhibitor of the cytochrome $b_6f$ plastoquinol oxidation site (see Fig. 5*B*). Under control conditions, the area below the cytochrome *f* oxidation transients is proportional to the number of electrons stored in the electron donors between PSII and PSI, provided that PSII activity is absent. Indeed, because of the small difference in redox potential between the Rieske protein, cytochrome *f*, and plastocyanin, full oxidation of cytochrome *f* can only occur when all the reducing equivalents have been consumed to re-reduce $P_{700}^+$ generated by light. On the other hand, because addition of DBMIB inhibits oxidation of plastoquinol, the area below the cytochrome *f* oxidation transients measured in the presence of this compound is proportional only to the number of PSI donors located downstream of the cytochrome $b_6f$ complex. Therefore, it may be used as an inter-

nal standard to calculate the size of the plastoquinone pool (see also "Experimental Procedures"). We found a significant (~30%) decrease in the number of plastoquinones available for cytochrome $b_6f$ catalysis in the mutant, when compared with the wild type.

To further assess whether the size of the free plastoquinone pool is changed in the mutant, a new strain (*menD1-QDO*) was generated by crossing the *menD1* mutant with *QDO*, a *Chlamydomonas* strain lacking the cytochrome $b_6f$ complex (41). The absence of the cytochrome $b_6f$ is required because the fluorescence emission in WT and the *menD1* strains reaches a steady state level ($F_{stat}$) upon illumination, which is well below the $F_{max}$ level attained in the presence of DCMU (Fig. 1*B*). This is because of the concomitant reduction and oxidation of the PSII acceptor pool, which ultimately prevents any assessment of the size of the plastoquinone pool by fluorescence measurements. In contrast, the plastoquinone pool reduced by PSII cannot be oxidized by PSI in the *QDO* and *menD1-QDO* double mutant strains because of the absence of the cytochrome $b_6f$ complex. Therefore, the fluorescence yield rises continuously upon illumination until it reaches the level obtained with DCMU (Fig. 5*C*). Similar to the case of the cytochrome *f* oxidation experiment, the area above the fluorescence curve is proportional to the number of electrons that have to be transferred to reach the $F_{max}$ level (42). Because a single photochemical act is needed to reduce $Q_A$ in the presence of DCMU, the ratio between the areas above the curves obtained in the absence and presence of DCMU yields the number of electrons that can be injected downstream of PSII in a cytochrome $b_6f$-lacking mutant, which equals twice the number of plastoquinone molecules per PSII.

The comparison between the *QDO* strain, used as reference strain, and *menD1-QDO* showed that the overall area was reduced in the latter. Yet a larger number of plastoquinone molecules per PSII could be calculated after normalization to the area determined in the presence of DCMU (8.7 ± 0.5 per PSII in the *menD1-QDO* and 5.7 ± 0.7 in the *QDO*). However, as the number of active PSII is also reduced in the *menD1* mutant, the increased plastoquinone/PSII ratio may still be consistent with a reduction of the total size of the plastoquinone pool, as suggested by the cytochrome *f* kinetics discussed above. To test this hypothesis, we titrated the number of active PSII complexes in the *QDO* strain by adding sub-stoichiometric amounts of DCMU to the *QDO* cells, to obtain in the *QDO* strain the same reduced PSII activity of the *menD1-QDO* mutant. Measurement of the number of plastoquinone molecules available per PSII in the QDO strain under these conditions revealed that it almost doubled (10.5 ± 0.5 per PSII). Thus we conclude that the total number of free plastoquinones is decreased in the membranes of the *MenD1-QDO* mutant (and therefore in the *menD1* mutant). Although this is not a proof, the data are consistent with the withdrawal of two plastoquinone molecules per photosynthetic electron transport chain.

*The Defect in the Phylloquinone Biosynthetic Pathway Has a Negative Impact on the Synthesis of PSII Subunits*—It was shown that in the *Synechocystis* sp. PCC 6803 strain lacking *menD*, the amount of PSI is lower than in wild-type cells (2, 3). We therefore tested whether the level of the different photosynthetic complexes in the *menD1* mutant was altered by immunoblotting of total proteins extracted from cells in exponential phase. As shown in Fig. 6*A*, no difference between *menD1* mutant and wild-type cells could be observed for subunits of PSI, the cytochrome $b_6f$ complex, ATP synthase, LHCI, LHCII, and ribulose-bisphosphate carboxylase/oxygenase. Surprisingly, a significant decrease in the accumulation of the reaction center subunits of PSII, D1, D2, and CP47 and of Oee1 and Oee2 was observed. The level of D1 protein in the mutant was decreased to 40% as compared with wild type (Fig. 6*B*). However, this decrease no longer occurred when total proteins were extracted from cells in stationary phase (Fig. 6*C*). Neither did it occur in the rescued strain *menD1R* (Fig. 6*C*). To test whether the decrease of PSII may be due to ROS, cells were grown under low oxygen pressure. Under these conditions the decrease of PSII was still observed (Fig. 6*C*). In agreement with these results, measurements of PSI/PSII activities revealed a large decrease of PSII activity compared with PSI activity in *menD1* cells (Fig. 6*D*; Table 1). PSII activity was restored to the wild-type level in the rescued strain *menD1R* (Fig. 6*D*; Table 1). Although a slight decrease in PSI activity was detected by electrochromic shift measurements (Fig. 6*D*), no decrease in PSI activity was apparent when its activity was measured by oxygen uptake through methyl viologen (Table 1). This suggests that although charge separation is affected in *menD1*, this step is not rate-limiting for the overall PSI activity.

The specific decrease of PSII protein levels in cells grown in exponential phase suggested that it was because of a defect in its synthesis. Thus, we first checked the level of *psbA* mRNA, a representative mRNA of PSII in the *menD1* mutant compared with the wild-type, by RNA blot analysis of total RNA extracted from cells in exponential phase with a *psbA*-specific probe. Fig. 7*A* shows that the *psbA* mRNA accumulates to the same extent in *menD1* as in wild-type cells. To test if the synthesis of PSII subunits was affected in the mutant, cells were labeled with $Na_2{}^{35}SO_4$ for 10 min in the presence of cycloheximide, an inhibitor of cytosolic translation. Total cell proteins were then analyzed by SDS-PAGE and autoradiography. It can be seen in Fig. 7*B* that there was a significant decrease in protein labeling in the mutant compared with the wild type and the rescued mutant, in particular the synthesis of D1 protein was significantly reduced. These data suggest that the decrease in D1 observed in the mutant by immunoblotting is because of a defect in the translation of *psbA* mRNA.

To exclude the possibility of a defect in the stability of the D1 protein, we also performed a short pulse labeling followed by a chase of 10 and 60 min. No degradation could be observed under these conditions (data not shown). The stability of D1 protein in the mutant was further tested by adding chloramphenicol to the cultures. Wild-type and *menD1* cells were grown under 6 $\mu$E $m^{-2}$ $s^{-1}$ light in exponential phase, and the cultures were divided into two parts, one supplemented with chloramphenicol to inhibit chloroplast protein synthesis and the other without drug. Samples of cells were then removed 1, 3, 5, and 8 h after the addition of chloramphenicol. Total proteins were then analyzed by immunoblotting using a D1 antibody. Addition of chloramphenicol led to a slight decrease of D1 after 5 h, in both wild-type and mutant extracts as compared with cells grown in the absence of chloramphenicol (Fig. 7*C*). There

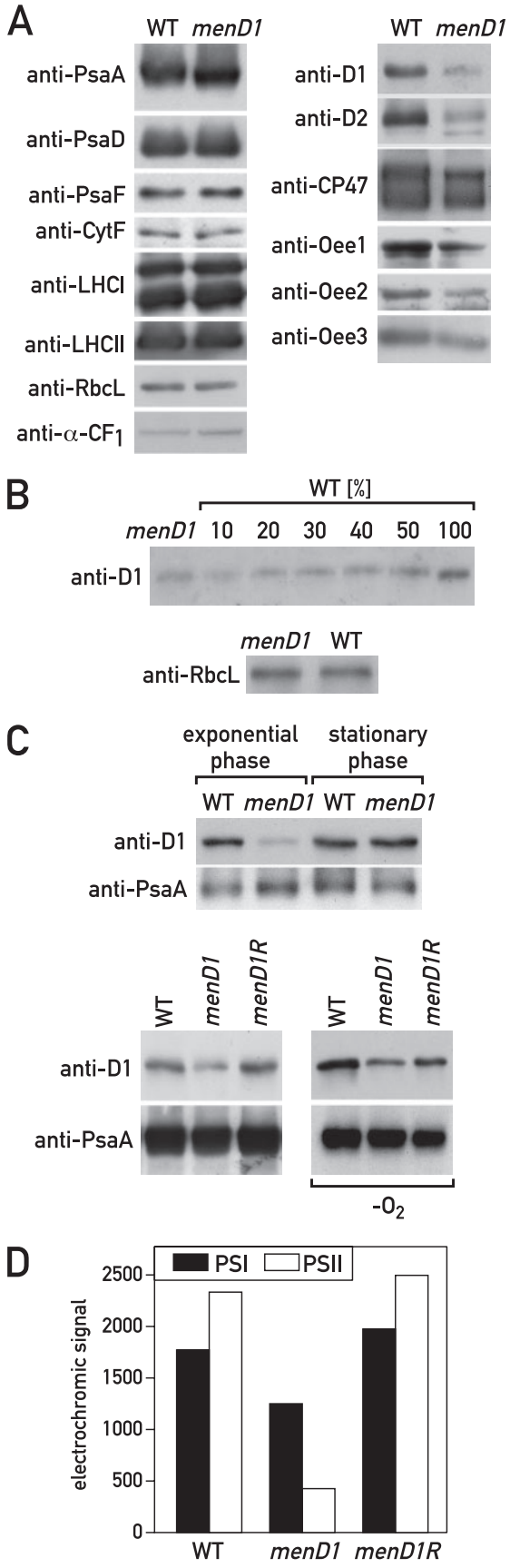


FIGURE 6. *A,* immunoblots of total wild-type and *menD1* cell extracts. The antibodies used are indicated. *B,* wild-type dilution series was used to estimate the amount of D1 protein in *menD1* using D1 antibodies. *C, upper,* the level of D1 protein is decreased in *menD1* cells in exponential phase but reaches wild-type levels in cells in stationary phase. *Lower,* the level of D1 protein is decreased in *menD1* cells both under aerobic conditions (*left*) and under reduced oxygen pressure (*right*) under 6 $\mu$E $m^{-2}$ $s^{-1}$ light. Immunoblots were performed with total cell extracts from cultures of wild-type, *menD1*, and *menD1R* cells. *D,* PSII activity is reduced in *menD1*. PSI and PSII photosynthetic activity was estimated in wild-type, *menD1,* and *menD1R* cells grown under 6 $\mu$E $m^{-2}$ $s^{-1}$ light by measurements of the induced charge separation through the electrochromic shift (see "Experimental Procedures").

**TABLE 1**

**Measurements of PSII and PSI activity**

Activity measurements were performed with cells from WT, *menD1*, and *menD1R*. PSI activity was measured in cells disrupted by sonication (30 $\mu$g/ml Chl). Oxygen uptake was measured with a Clark-type oxygen electrode in the presence of sodium ascorbate and 2,6-dichlorophenolindophenol as electron donors and methyl viologen. Oxygen evolution activity of PSII was measured in whole cells (10 $\mu$g/ml Chl) with a Clark-type oxygen electrode in the presence of phenyl-*p*-benzoquinone as electron acceptor and DBMIB. For details see "Experimental Procedures." Numbers in parentheses indicate the number of independent measurements. PSI and PSII measurements were done under 20 and 250 $\mu$mol $m^{-2}$ $s^{-1}$ red light, respectively.

| Strain | PSI activity | PSII activity |
|---|---|---|
| | *$\mu$mol $O_2$/mg Chl/h* | *$\mu$mol $O_2$/mg Chl/h* |
| WT | 19.0 ± 1.9 (3) | 23.6 ± 1.6 (6) |
| *menD1* | 24.4 ± 2.4 (3) | 12.6 ± 1.7 (5) |
| *menD1R* | 21.8 ± 1.7 (3) | 24.5 ± 0.7 (6) |

was no evidence for enhanced degradation of D1 in *menD1*. We conclude from these data that the low amount of D1 protein level observed in the *menD1* mutant is due mainly to a defect in the synthesis of the protein and not to a decrease in its stability.

To test whether the altered redox state of the plastoquinone pool could be responsible for the defect in the synthesis of PSII subunits, we used the electron transport inhibitors DCMU and DBMIB, which lead to oxidation and reduction of the plastoquinone pool in the light, respectively. Wild-type and mutant cultures in exponential phase were divided in three parts, one without inhibitor, one supplemented with DBMIB, and the last with DCMU. Cells were collected after 8 h, and total proteins were extracted and analyzed by immunoblotting with a D1 antibody. Neither DBMIB nor DCMU had any effect on the accumulation of D1 protein in mutant and wild-type cells, indicating that the redox state of the plastoquinone pool does not have a significant effect on D1 accumulation (supplemental Fig. S2).

If the reduced size of the free plastoquinone pool is because of the replacement of phylloquinone by plastoquinone in PSI, one might expect that in the absence of PSI the size of the free plastoquinone pool would be restored and PSII levels would increase. This was tested by constructing the *menD1-tab2-F14* double mutant from a cross between *menD1* and the PSI mutant *tab2-F14* (34). Immunoblot analysis with D1 antibodies revealed that the PSII level in *menD1-tab2-F14* was the same as in *menD1* (supplemental Fig. S3). However, we noticed that the level of PSII was also reduced in the parental strain *tab2-F14* under the conditions used. The same decrease in PSII was observed with *Im1*, another PSI mutant.[4] It was therefore not possible to test for the restoration of PSII because of the counter-acting effect observed in the PSI mutants.

[4] V. Winter and J. D. Rochaix, unpublished results.

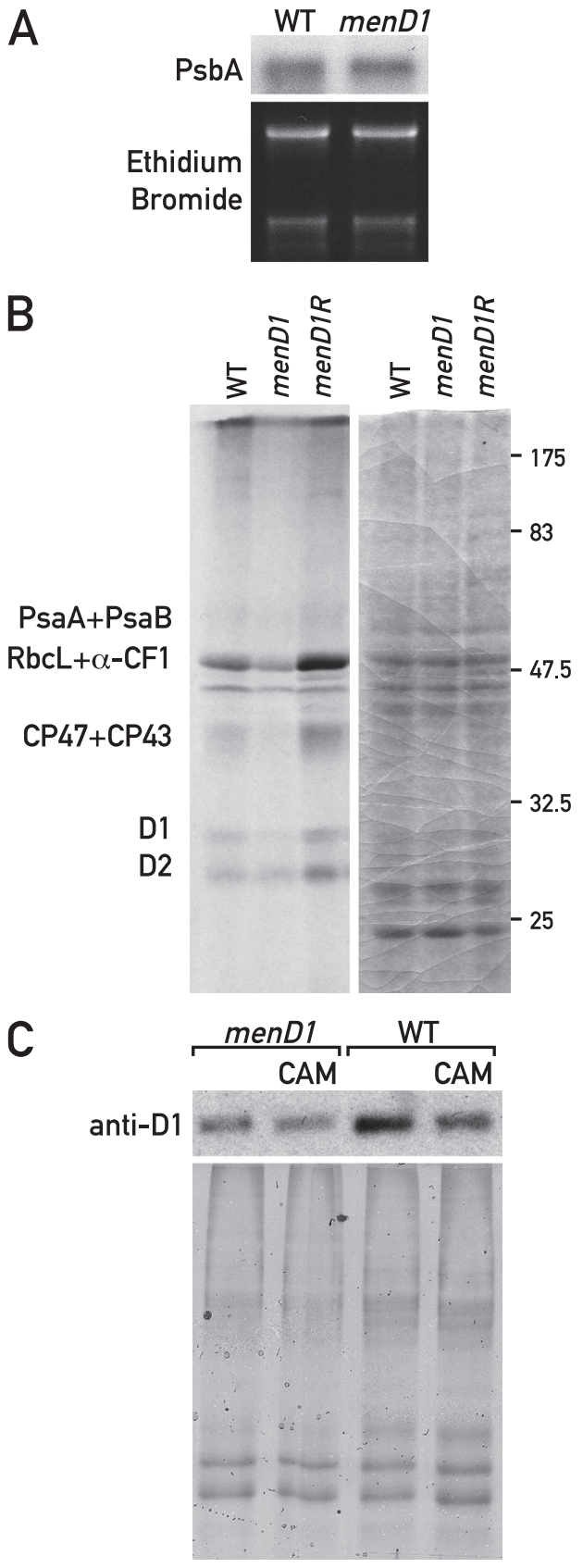


FIGURE 7. *A, psbA* mRNA accumulates normally in *menD1* cells. Total RNA from wild-type and *menD1* cells was isolated, fractionated by agarose gel electrophoresis, blotted onto nylon filter paper, and hybridized with a *psbA* probe. The *lower part* shows the ethidium bromide staining of rRNA. *B,* pulse labeling of proteins from wild-type and *menD1* cells for 10 min with [$^{35}$S]sulfate in the presence of cycloheximide. *Left,* autoradiograph; *right,* Coomassie Blue staining. *C,* stability of D1 protein is not affected in *menD1* cells compared with wild type. Cells were grown in the presence or absence of chloramphenicol (*CAM*). Total protein was extracted, fractionated by SDS-PAGE, and immunoblotted with D1 antibodies (*upper part*). The *lower part* shows the gel stained with Coomassie Blue.

## DISCUSSION

*The menD1 Mutant Is Deficient in Phylloquinone Synthesis*—We have used insertion mutagenesis in *Chlamydomonas* to isolate the *menD1* mutant. This mutant is light-sensitive and does not grow photoautotrophically under moderate light (60 $\mu$E $m^{-2}$ $s^{-1}$). Analysis of the insertion site revealed that the inactivated gene corresponds to *MenD* coding for SHCHC synthase, which catalyzes the first specific step in the phylloquinone biosynthesis pathway. This was further confirmed by showing that the mutant phenotype cosegregates with the insertion during crosses. The wild-type phenotype could be restored upon transformation of the mutant with the wild-type *MenD* gene of *Chlamydomonas*. Mass spectrometric measurements revealed that phylloquinone is not detectable in thylakoid membranes from *menD1* but could be readily identified in the wild type. The plastoquinone content was the same in the mutant and in the wild type. Moreover, addition of phylloquinone to the growth medium restored growth under high light. Taken together these data indicate that the *menD1* mutant is unable to produce phylloquinone and that, as in cyanobacteria, there is no alternative biosynthetic route that circumvents SHCHC synthase in *Chlamydomonas*.

In cyanobacteria it was shown that recruitment of plastoquinone into the $A_1$ site of PSI occurs in the absence of phylloquinone and that plastoquinone can function as an intermediate in electron transfer between $A_0$ and the iron-sulfur center $F_X$ (2–4, 16, 36). Our analysis by differential absorption spectroscopy suggests that the same substitution occurs in the *menD1* mutant of *Chlamydomonas*. The absorbance change 10 ns after the actinic flash relative to wild type decreased in the 380 nm region corresponding to phylloquinone and increased in the 320 nm region corresponding to plastoquinone (Fig. 4*B*). Moreover, under aerobic conditions the absorption change at 320 nm decayed with a half-time of 6 $\mu$s (Fig. 4*B*), which indicates that the forward electron transfer to the iron sulfur center $F_X$ is slowed down at least 40-fold in *MenD1* compared with wild type. Similar observations have been made in *Synechocystis* sp. PCC 6803 lacking phylloquinone where the half-time of reoxidation of plastosemiquinone (~15 $\mu$s) is significantly slower than that of the native phyllosemiquinone (~20 and ~200 ns) (16). This has been interpreted as resulting from the less negative redox potential of the $PQ^-$/PQ couple compared with that of $PhyQ^-$/PhyQ, which renders the electron transfer to $F_X$ thermodynamically unfavorable (43).

The existence of biphasic kinetics of quinone oxidation has been interpreted as the signature of a bi-directional electron transfer process in PSI. In this respect it is interesting to note that the oxidation of plastosemiquinone is essentially monophasic in *menD1*. The difference in the rates of electron transfer between the two phylloquinones and the $F_X$ iron-sulfur cluster has been accounted for by Agalarov and Brettel (44) by

the fact that the fast phase is associated with little activation energy in contrast to the slow phase. With the replacement of phylloquinone by plastoquinone, both phases are expected to be uphill in energy and thus slower, as proposed by Shinkarev *et al.* (43), explaining why the difference in their rate might be less pronounced.

It is notable that $P_{700}^+$ decayed with a similar half-time than the 320 nm decay ascribed to the reduction of plastosemiquinone. Such a half-time is consistent with the reduction of $P_{700}^+$ by prebound plastocyanin (48). However, the similarity between the decay rates of the signals ascribed to plastosemiquinone ($PQ^-$) and $P_{700}^+$ could also be interpreted as a charge recombination of the $P_{700}^+PQ^-$ radical pair. However, this possibility is highly unlikely because such a charge recombination process would result in the decay of the transmembrane electric field induced by the $P_{700}^+PQ^-$ dipole. Such decay does not occur in *menD1* because the lifetimes for the electrochromic band shift induced by the electric field are similar in the control and mutant strains. Moreover, if forward electron transfer to the iron-sulfur cluster were blocked by the replacement of phylloquinone by plastoquinone, the overall electron transfer activity of the photosynthetic chain would be severely impaired, which is clearly not the case for *menD1*.

However, charge recombination appears to occur upon prolonged anaerobiosis when the rate of $P_{700}^+$ reduction is considerably increased. In intact cells, anaerobiosis is known to promote the reduction of the plastoquinone pool. It is thus conceivable that in the *menD1* mutant, plastoquinone bound in the $A_1$ site may exchange with the plastoquinone pool and thus be reduced under anaerobic conditions. The question as to whether plastoquinol may occupy or not the $A_1$ site remains open because either an empty site or a bound plastoquinol would prevent forward electron transfer from $A_0^-$. Clearly, no such plastoquinol release from PSI is seen after short periods of anaerobiosis, because we observed that the size of the free plastoquinone pool is decreased in *menD1*. On the other hand, the ability of a bound plastoquinone to leave its site and exchange with a free plastoquinone from the pool agrees with the observation that the limited growth rate under high light conditions could be rescued by addition of phylloquinone. Yet the experiments performed in Fig. 4*C* suggest that this exchange is extremely slow and is probably not of physiological relevance.

*Reduced Size of the Free Plastoquinone Pool in menD1*—Based on both measurements of cytochrome *f* oxidation rates (Fig. 5*B*) and fluorescence transients (Fig. 5*C*), we estimate the size of the plastoquinone pool of *menD1* to be reduced by 20–30% compared with the wild type. This is likely due to the recruitment of plastoquinone in PSI. The replacement of phylloquinone by plastoquinone in photosystem I still allows for photosynthetic electron flow (Fig. 1*B*). However, it appears that the altered PSI is not fully functional, leading to impaired growth under high light or on minimal medium (Fig. 1*A*). The absence of phylloquinone in the *menD1* mutant does not affect the level of PSI. This result is surprising given the fact that minor changes in the reaction center of PSI can strongly destabilize the complex (45) and that in *Synechocystis* loss of phylloquinone significantly lowers the ratio between PSI and PSII. One possible explanation for this difference would be the different composition of PSI in the two organisms. Indeed, some of the PSI subunits from *Chlamydomonas* (PsaG, PsaH, and PsaN) are missing in cyanobacteria. The function of PsaG is not clear, but it is known that PsaH is involved in the stabilization of the PSI complex, and PsaN is involved in PSI trimer formation (46). Thus, the presence of these subunits in *Chlamydomonas* could improve the stability of PSI-containing plastoquinone. However, this does not explain why PSI lacking phylloquinone is considerably more stable in *Chlamydomonas* than in *Arabidopsis* where it accumulates to only 5–15% (7). One possibility is that the insertion of plastoquinone into PSI is less efficient in plants.

It is well established that most mutants affected in photosynthesis are sensitive to high light, especially the PSI mutants. However, the analysis of PSI mutants of *Chlamydomonas* has shown that the relationship between diminished photosynthetic activity and impaired growth under high light is not straightforward. For example, some *psaC* mutants are highly sensitive to light but display only a slight decrease in the NADP photoreduction, whereas the *3bF* mutant lacking the PsaF subunit is less affected in light tolerance but shows a large decrease in NADP photoreduction (47). It is possible that the lower redox potential of the $PQ^-$/PQ couple may enhance accumulation of the semiquinone species at the $A_1$ site, promoting the formation of ROS in *menD1*. This possibility is compatible with the observation that the light sensitivity is abolished and the growth on minimal medium restored when the cells are grown under reduced oxygen pressure.

*Relationship between Loss of Phylloquinone and Reduced Levels of PSII*—The decrease of PSII in the *menD1* mutant is also observed in other *Chlamydomonas* mutants lacking PSI. It is possible that as indicated above PSI in *menD1* generates ROS, which leads to photoinhibition. However, the production of ROS cannot explain the decline of PSII in *menD1* because it still occurs under low oxygen pressure (Fig. 6*C*). In addition, our results differ considerably from those obtained with phylloquinone-deficient cyanobacteria and land plants. In *Synechocystis* sp. PCC 6803 deficient in *menD,* the ratio of PSI to PSII is significantly reduced relative to wild type (2, 3), whereas the opposite is found in *C. reinhardtii*. In *A. thaliana* loss of phylloquinone leads to a drastic reduction in PSI and to a significant decrease in plastoquinone (6, 7). Similar differences between *Chlamydomonas* and *Arabidopsis* have been observed in other cases. As an example loss of PsaF in *C. reinhardtii* has no apparent effect under normal light conditions (48), whereas in *A. thaliana* absence of PsaF strongly destabilizes the PSI complex and prevents photoautotrophic growth (49). These differences might be explained by the presence of an efficient clearing system in land plants, which recognizes minor conformational changes of the photosynthetic complexes and induces their degradation.

The decreased size of the free plastoquinone pool may lead to a reduced occupancy of the $Q_A$ and $Q_B$ pockets in PSII. Such a defect in D2 $Q_A$ cofactor assembly could reduce D1 synthesis through the CES (controlled by epistasy of synthesis) process, which makes D1 translation dependent on the presence of its partner D2 subunit in the thylakoid membrane (50). Previous studies have revealed the existence of diffusion domains for the

quinones that exchange protons and electrons only on a very slow time scale (51). Because of variable PSII/quinone stoichiometries in each domain, a non-negligible fraction of PSII may not be loaded with plastoquinone at the $Q_B$ site. This fraction may be further increased in the *menD1* mutant because of the lower number of freely diffusing quinones. This may affect PSII levels. Indeed, it has been shown that PSII degradation can also occur at low light intensities through high turnover of the D1 protein because of back electron flow and charge recombination between the $Q_B^-$ or $Q_A^-$ semiquinone acceptors and the PSII donor side (52). This gives rise to ROS and causes oxidative damage, which is prevented under anaerobic conditions. In this respect it is interesting that translation of the large subunit of ribulose-bisphosphate carboxylase/oxygenase has been shown to be affected by ROS (53). The D1 breakdown appears to proceed in two steps, first photoinactivation of D1 and subsequently D1 degradation (54). The second step requires that the $Q_B$ site be occupied by plastoquinone. It is impaired by a high plastoquinol to plastoquinone ratio. However, the case of the *menD1* mutant differs in two important aspects. First, the decrease of PSII occurs to the same extent under low oxygen pressure; and second, it is because of a diminished rate of synthesis of D1 rather than to D1 degradation as measured by pulse labeling, pulse-chase experiments, and D1 stability measurements. Although synthesis of D1 appears to be the principal target, accumulation of the other PSII proteins is also limited because any PSII core protein produced in excess amounts relative to D1 will be degraded (1).

Alternatively, D1 synthesis may be influenced by the redox state of the plastoquinone pool. Although the impact of the redox state of the plastoquinone pool on gene expression has been studied intensively, the chloroplast signaling chain is still poorly understood, especially because data are often contradictory or inconclusive (for review see Ref. 55). A complex of four proteins that binds the 5′-untranslated region of the *psbA* mRNA has been identified in *Chlamydomonas* (56, 57). This complex regulates the rate of translation initiation of the mRNA under different redox conditions (58). However, in our case neither DCMU nor DBMIB had any detectable effect on PSII accumulation in the light suggesting that this particular process is not controlled by the redox state of the plastoquinone pool.

Clearly, our case may be different, as no studies have been performed on how the chloroplast translation machinery senses and responds to changes in the size of the free plastoquinone pool. Finally, it is possible that alterations in electron transfer within PSI, as caused by the replacement of phylloquinone by plastoquinone, may directly influence D1 synthesis through a still unknown signaling chain.

*Acknowledgments—We thank Nicolas Roggli for drawings and photography, Dr. Jon Falk for samples of plastoquinone, and Michel Goldschmidt-Clermont for critical reading of the manuscript.*

## REFERENCES


1. Barkan, A., and Goldschmidt-Clermont, M. (2000) *Biochimie* (*Paris*) **82,** 559–572
2. Johnson, T. W., Shen, G., Zybailov, B., Kolling, D., Reategui, R., Beauparlant, S., Vassiliev, I. R., Bryant, D. A., Jones, A. D., Golbeck, J. H., and Chitnis, P. R. (2000) *J. Biol. Chem.* **275,** 8523–8530
3. Johnson, T. W., Zybailov, B., Jones, A. D., Bittl, R., Zech, S., Stehlik, D., Golbeck, J. H., Chitnis, P. R., van der Est, A., Zech, S. G., Teutloff, C., Shen, G., Kolling, D., Reategui, R., Beauparlant, S., Vassiliev, I. R., and Bryant, D. A. (2001) *J. Biol. Chem.* **276,** 39512–39521
4. Zybailov, B., van der Est, A., Zech, S. G., Teutloff, C., Johnson, T. W., Shen, G., Bittl, R., Stehlik, D., Chitnis, P. R., Golbeck, J. H., Kolling, D., Reategui, R., Beauparlant, S., Vassiliev, I. R., Bryant, D. A., and Jones, A. D. (2000) *J. Biol. Chem.* **275,** 8531–8539
5. Sakuragi, Y., Zybailov, B., Shen, G., Jones, A. D., Chitnis, P. R., van der Est, A., Bittl, R., Zech, S., Stehlik, D., Golbeck, J. H., and Bryant, D. A. (2002) *Biochemistry* **41,** 394–405
6. Shimada, H., Ohno, R., Shibata, M., Ikegami, I., Onai, K., Ohto, M. A., Takamiya, K., Wakabayashi, H., Onodera, K., Yamato, S., Shimada, K., Iwaki, M., Takahashi, M., Takahashi, Y., and Itoh, S. (2005) *Plant J.* **41,** 627–637
7. Gross, J., Cho, W. K., Lezhneva, L., Falk, J., Krupinska, K., Shinozaki, K., Seki, M., Herrmann, R. G., and Meurer, J. (2006) *J. Biol. Chem.* **281,** 17189–17196
8. Diner, B. A., Schlodder, E., Nixon, P. J., Coleman, W. J., Rappaport, F., Lavergne, J., Vermaas, W. F., and Chisholm, D. A. (2001) *Biochemistry* **40,** 9265–9281
9. Iwata, S., and Barber, J. (2004) *Curr. Opin. Struct. Biol.* **14,** 447–453
10. Nelson, N., and Ben-Shem, A. (2005) *BioEssays* **27,** 914–922
11. Joliot, P., and Joliot, A. (1999) *Biochemistry* **38,** 11130–11136
12. Guergova-Kuras, M., Boudreaux, B., Joliot, A., Joliot, P., and Redding, K. (2001) *Proc. Natl. Acad. Sci. U. S. A.* **98,** 4437–4442
13. Dashdorj, N., Xu, W., Cohen, R. O., Golbeck, J. H., and Savikhin, S. (2005) *Biophys. J.* **88,** 1238–1249
14. Bautista, J. A., Rappaport, F., Guergova-Kuras, M., Cohen, R. O., Golbeck, J. H., Wang, J. Y., Beal, D., and Diner, B. A. (2005) *J. Biol. Chem.* **280,** 20030–20041
15. Meganathan, R. (2001) *Vitam. Horm.* **61,** 173–218
16. Semenov, A. Y., Vassiliev, I. R., van Der Est, A., Mamedov, M. D., Zybailov, B., Shen, G., Stehlik, D., Diner, B. A., Chitnis, P. R., and Golbeck, J. H. (2000) *J. Biol. Chem.* **275,** 23429–23438
17. Fleischmann, M. M., Ravanel, S., Delosme, R., Olive, J., Zito, F., Wollman, F. A., and Rochaix, J. D. (1999) *J. Biol. Chem.* **274,** 30987–30994
18. Depège, N., Bellafiore, S., and Rochaix, J. D. (2003) *Science* **299,** 1572–1575
19. Li, Y., Lucas, M. G., Konovalova, T., Abbott, B., MacMillan, F., Petrenko, A., Sivakumar, V., Wang, R., Hastings, G., Gu, F., van Tol, J., Brunel, L. C., Timkovich, R., Rappaport, F., and Redding, K. (2004) *Biochemistry* **43,** 12634–12647
20. Harris, E. H. (1989) *The Chlamydomonas Source Book: A Comprehensive Guide to Biology and Laboratory Use*, pp. 1–790, Academic Press, Inc., San Diego
21. Kindle, K. L. (1990) *Proc. Natl. Acad. Sci. U. S. A.* **87,** 1228–1232
22. Sambrook, J., Fritsch, E. F., and Maniatis, T. (1989) *Molecular Cloning: A Laboratory Manual*, 2nd Ed., Cold Spring Harbor Laboratory Press, Cold Spring Harbor, NY
23. Boudreau, E., Takahashi, Y., Lemieux, C., Turmel, M., and Rochaix, J.-D. (1997) *EMBO J.* **16,** 6095–6104
24. Berthold, D. A., Best, B. A., and Malkin, R. (1993) *Plant Mol. Biol. Rep.* **11,** 338–344
25. Béal, D., Rappaport, F., and Joliot, P. (1999) *Rev. Sci. Instrum.* **70,** 202–207
26. Joliot, P., Beal, D., and Joliot, A. (2004) *Biochim. Biophys. Acta* **1656,** 166–176
27. Joliot, P., and Joliot, A. (1992) *Biochim. Biophys. Acta* **1102,** 53–61
28. Finazzi, G., Furia, A., Barbagallo, R. P., and Forti, G. (1999) *Biochim. Biophys. Acta* **1413,** 117–129
29. Schliephake, W., Junge, W., and Witt, H. T. (1968) *Z. Naturforsch. Sect. B Chem. Sci.* **23,** 1571–1578
30. Bennoun, P., and Joliot, A. (1969) *Biochim. Biophys. Acta* **189,** 85–94
31. Fischer, N., Setif, P., and Rochaix, J. D. (1997) *Biochemistry* **36,** 93–102
32. Merendino, L., Falciatore, A., and Rochaix, J. D. (2003) *Plant Mol. Biol.* **53,** 371–382
33. Durrant, I. (1990) *Nature* **346,** 297–298

34. Dauvillee, D., Stampacchia, O., Girard-Bascou, J., and Rochaix, J. D. (2003) *EMBO J.* **22,** 6378–6388
35. Takahashi, Y., Goldschmidt-Clermont, M., Soen, S. Y., Franzen, L. G., and Rochaix, J. D. (1991) *EMBO J.* **10,** 2033–2040
36. Johnson, T. W., Naithani, S., Stewart, C., Zybailov, B., Jones, A. D., Golbeck, J. H., and Chitnis, P. R. (2003) *Biochim. Biophys. Acta* **1557,** 67–76
37. Bensasson, R., and Land, E. J. (1973) *Biochim. Biophys. Acta* **325,** 175–181
38. Bottin, H., and Sétif, P. (1991) *Biochim. Biophys. Acta* **1057,** 331–336
39. Warren, P. V., Golbeck, J. H., and Warden, J. T. (1993) *Biochemistry* **32,** 849–857
40. Finazzi, G., Rappaport, F., Furia, A., Fleischmann, M., Rochaix, J. D., Zito, F., and Forti, G. (2002) *EMBO Rep.* **3,** 280–285
41. Kuras, R., and Wollman, F. A. (1994) *EMBO J.* **13,** 1019–1027
42. Delepelaire, P., and Bennoun, P. (1978) *Biochim. Biophys. Acta* **502,** 183–187
43. Shinkarev, V. P., Zybailov, B., Vassiliev, I. R., and Golbeck, J. H. (2002) *Biophys. J.* **83,** 2885–2897
44. Agalarov, R., and Brettel, K. (2003) *Biochim. Biophys. Acta* **1604,** 7–12
45. Redding, K., MacMillan, F., Leibl, W., Brettel, K., Hanley, J., Rutherford, A. W., Breton, J., and Rochaix, J. D. (1998) *EMBO J.* **17,** 50–60
46. Scheller, H. V., Jensen, P. E., Haldrup, A., Lunde, C., and Knoetzel, J. (2001) *Biochim. Biophys. Acta* **1507,** 41–60
47. Rochaix, J. D., Fischer, N., and Hippler, M. (2000) *Biochimie* (*Paris*) **82,** 635–645
48. Farah, J., Rappaport, F., Choquet, Y., Joliot, P., and Rochaix, J. D. (1995) *EMBO J.* **14,** 4976–4984
49. Haldrup, A., Simpson, D. J., and Scheller, H. V. (2000) *J. Biol. Chem.* **275,** 31211–31218
50. Minai, L., Wostrikoff, K., Wollman, F. A., and Choquet, Y. (2006) *Plant Cell* **18,** 159–175
51. Lavergne, J., and Joliot, P. (1991) *Trends Biochem. Sci.* **16,** 129–134
52. Keren, N., Berg, A., van Kan, P. J., Levanon, H., and Ohad, I. I. (1997) *Proc. Natl. Acad. Sci. U. S. A.* **94,** 1579–1584
53. Irihimovitch, V., and Shapira, M. (2000) *J. Biol. Chem.* **275,** 16289–16295
54. Zer, H., Prasil, O., and Ohad, I. (1994) *J. Biol. Chem.* **269,** 17670–17676
55. Pfannschmidt, T. (2003) *Trends Plant Sci.* **8,** 33–41
56. Danon, A., and Mayfield, S. (1991) *EMBO J.* **10,** 3993–4001
57. Danon, A., and Mayfield, S. P. (1994) *EMBO J.* **13,** 2227–2235
58. Trebitsh, T., Levitan, A., Sofer, A., and Danon, A. (2000) *Mol. Cell. Biol.* **20,** 1116–1123
59. Thompson, J. D., Higgins, D. G., and Gibson, T. J. (1994) *Nucleic Acids Res.* **22,** 4673–4680
60. Rappaport, F., Béal, D., Joliot, A., and Joliot, P. (2007) *Biochim. Biophys. Acta* **1767,** 56–65